EUROREGIO BNAM2022
Joint Acoustics Conference
9th-11th of May, Aalborg, Denmark

Modeling of multiple reflections between noise barriers and trains using the boundary element method

Christian H. Kasess[1,*], **Thomas Maly**[2], **Wolfgang Kreuzer**[1]

[1]Acoustics Research Institute, Austrian Academy of Sciences, Vienna, Austria.

[2]Institute for Transportation, TU Wien, Vienna, Austria.

[*]christian.kasess@oeaw.ac.at

Abstract

While noise barriers are built to act as an acoustical barrier, they also cause an optical barrier effect, which could be reduced using transparent elements. Typically, such elements are acoustically highly reflecting. Unfortunately, in particular for railway traffic highly reflecting surfaces potentially reduce the insertion loss by multiple reflections between train and barrier. Current noise mapping methods such as the EU directive 2002/49/EC (Annex II) provide means to approximately consider such reflections. There is, however, the need for detailed investigations how the placement and dimensions of sound hard elements, the distance of the train to the barrier, the train cross-section, the distance of the observer, and other variables influence the insertion loss of the barrier. Measurements of passbys for 4 different barrier variants combining highly absorbing and reflecting materials were performed. These measurements provide the basis for the validation of the 2.5D boundary element calculations. In a next step, based on calculations of many different configurations a simplified, practical calculation model will be derived which may be used in noise mapping applications.

Keywords: noise barriers, railway traffic, reflecting elements, boundary element method, insertion loss.

1 Introduction

Noise barriers are an important tool for environmental noise control, in particular for traffic noise. However, in addition to the desired acoustical effect, noise barriers also are an optical barrier obstructing the view for passengers as well as for residents. Transparent elements could reduce this visual barrier effect. Typically, transparent elements for noise barriers are sound hard. The highly reflecting surfaces of common transparent barrier elements, however, pose a large problem in particular for railway traffic as they may produce considerable multiple reflections between train and barrier, potentially reducing the insertion loss of the barrier [1].

Current noise mapping methods such as the EU directive 2002/49/EC (Annex II) [2] provide means to approximately consider such multiple reflections including retrodiffraction assuming parallel planes and constant absorption over the entire height of the barrier. The main question being, whether the framework in the Annex II [2] is sufficient to deal with a variety of situations that occur in railway traffic where e.g. transparent elements are often placed only in the upper sections of the barrier. For example, in Morgan et al. [3] the effect of absorption and the train cross-section was investigated using the boundary element method (BEM) in 2D. They showed a large effect of absorption on the noise barrier which was larger for a box-shaped train than for a rounded vehicle body. This study, however, only considered barriers which were either absorbing or reflecting as a whole, although different barrier shapes were investigated. Recently, Bustos et al. [4] investigated the effect of mixing reflecting an absorbing parts on a noise barrier using a combined boundary element-finite element approach. There it was found, that the vertical placement, the barrier height as well as the distance of the

source to the barrier influence the insertion loss. However, for computational reasons both studies used pure 2D approaches which implies a fully coherent, infinitely long line source, which is computationally efficient but unrealistic. Furthermore, only overall changes are reported although it seems clear that frequency dependency effects play an important role. Finally, neither study was validated using measurements as for instance the study of Kirisits et al. [1] who investigated the influence of retrodiffraction on the calculation results, however, for highly absorbing noise barriers only. Thus, there is still the need for more detailed investigations how the placement and dimensions of sound hard elements, the distance of the train to the barrier, the train cross-section, the distance of the observer, and other variables influence the insertion loss of the barrier.

The work presented here aims at investigating the different factors systematically using the 2.5D BEM [5, 6]. The advantage of the 2.5D approach is, that under the assumption of a constant cross-section point sources as well as incoherent line sources can be modeled. To validate the computational approach extensive measurements campaign were carried out consisting of acoustic passby measurements of four different barrier variants combining highly absorbing and reflecting materials. Using the so determined source model calibration, simulations of many different configurations will be used to derive a simplified, practical calculation model which may be used in noise mapping applications.

2 Methods

2.1. Measurement setup

For the measurements a site was chosen, where two adjacent measurement cross-sections with and without a barrier were available and where the surroundings were essentially flat. The site was located close to Vienna along the eastern line. The noise barrier was a concrete noise barrier covered with a highly absorbing layer of wood-fibre concrete which was present on both sides of the barrier with a rippled diffuser profile oriented towards the train. The height of the barrier was 2 m above the top of the rail. The noise barrier's cross-section was placed 250 m away from the end of the barrier. A reference cross-section with unobstructed sound propagation was located 200 m away from the end of the barrier in the other direction.

The noise barrier cross-section was equipped with 9 microphones: 2 between train and noise-barrier (Pre-Sonus PRM-1, 1.2 m and 2.8 m above the top of the rail), 5 microphones at 7.5 m (G.R.A.S. 46AE, equally spaced heights from 1.2 m to 3.6 m above the top of the rail), and 2 microphones at 25 m (B&K UA-1404, heights 2.0 m and 4.5 m above the top of the rail). Two inductive wheel sensors (one per track) were used to determine the time of axle passbys as well as train speeds.

The reference cross-section was equipped with 2 microphones (G.R.A.S 46AE) located at the standard emission point (7.5 m, 1.2 m above the top of the rail) and in the upper 25 m position as in the noise barrier cross-section. In this cross-section train speeds and axle spacings were determined using two light barriers. The sampling rate of the acoustic measurements in the barrier cross-section was 48 kHz and in the reference section (due to different recording hardware) 51.2 kHz which were resampled to 48 kHz for further analysis. For manual analysis of train types and vehicle composition of freight trains all train passbys were recorded with a video camera. To ensure the comparability of the noise emissions between the cross-sections rail roughness and track decay rates of the rails of both tracks and cross-sections were measured.

2.2. Noise barrier modifications

In order to investigate the effect of highly reflective material, 40 plywood panels (27mm thick, 3-layers, spruce, covered with a thin layer of melamine resin) were used. The panels were placed in front of the rippled absorber using a custom made steel construction. There was a distance of around 6 cm between absorber and wood panel. Each panel was 2.5 m long and 1 m high. A total of 100 m of the noise barrier were covered, centered around the measurement cross-section. Three different panel placements were investigated: 1) panels were placed at the top of the barrier such that the upper meter was covered (Fig. 1); 2) panels were placed 0.5 m below the

barrier edge; 3) starting from state 2, every second panel was removed. For the top positioning (variant 1), the gap on top of the barrier due to the distance between barrier and panels was covered using small wooden panels to avoid absorption at the barrier edge which can be seen in Fig. 1.

Figure 1: Modified noise barrier. Shown is the upper panel configuration.

2.3. Boundary element method

Boundary element calculations were performed using the 2.5D BEM [5, 6]. The assumption is, that the scatterer is infinitely long and has a constant cross-section. However, in contrast to pure 2D BEM the source can be a point or an incoherent line source. The ballasted track was modeled using a 3-layer impedance model [7]. The highly absorbing noise barrier was defined from absorption measurement using real (zero phase) impedance values. The absorption values at high frequencies were around 0.9. Similarly, the wood panels were modeled using absorption coefficients for OSB boards [8]. A number of different source positions and train cross-sections were modeled (Fig. 2 shows the passenger train). Source positions were located at the top of the rail and at roughly the center of the wheel (points in Fig. 2). Omnidirectional as well as dipole sources were investigated. Point sources were placed at a spacing of 1.25 m along the track. The energy was integrated using a Simpson rule to obtain the result of an incoherent line source of about 1.5 times the length of the train. Due to the restrictions on the scatterer for the 2.5D BEM a number of important simplifications had to be applied. First, the bogies and wheels cannot be modeled properly, thus similar to previous work these lower parts of the wagons were not present in the model [9, 10]. Second, for the setting with alternating panels computationally involved methods utilizing the periodic structure based on the Floquet transform e.g. [11] were not considered. Instead, a somewhat diffuse field between barrier and train was assumed and the frequency dependent mean of the absorption of the wooden panels and the noise barrier was used to model the panel absorption for the alternating case. Third, gaps between wagons cannot be modeled and were thus ignored. This is mostly relevant for certain freight trains. Fourth, the steel structure on which the panels were mounted was not considered.

2.4. Data analysis

During regular operation, various train types were recorded including passenger trains, commuter trains, as well as a variety of different freight trains. For the latter the type of vehicle body contained cylindrical tanks, container or other wagons with vertical reflecting structures, car transporters, and other specialized types of wagons. Flat wagons (e.g. for containers or wood) not carrying any load were also observed.

The main focus here is on passenger and commuter trains due to their homogenous exterior shape, however two types of freight trains are also reported. For the passenger trains the procedure was to define a segment of the recording on the basis of the axles such that acoustic effects of the ends of the train are reduced. The passenger train (4 to 6 passbys per barrier configuration, speeds from 119 to 140 km/h) was about 200 m long

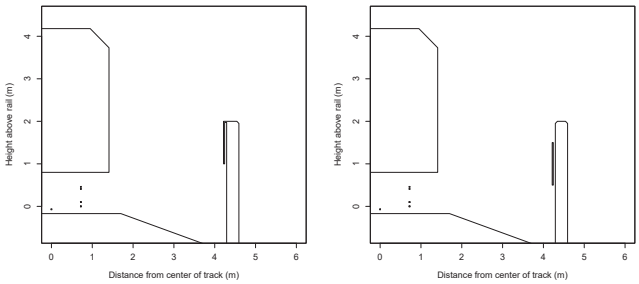

Figure 2: Cross-sections used for the simulation of the passenger train. The left panel shows the upper panel configuration, the right panel the middle configuration.

with a locomotive located at one end. At both ends 12 axles were ignored considering only the middle section. For the two types of observed commuter trains (6 to 21 passbys per configuration, length of 140 m in total, speeds from 130 to 140 km/h) 8 axles were ignored at each end. For freight trains, the video recordings were used to identify sections of freight trains with homogenous wagon types.

Using the Large Time-Frequency Analysis Toolbox (LTFAT, [12]) spectrograms were generated (function *dgtreal*, 4096 frequency channels, 1000 samples hop size). One-third octave band spectra for each point in time were generated by energetically summing up the respective frequency bins. Using the axle timing data the first and last axle of the middle segment were determined and an energetic average over the so defined section was calculated. For freight trains, due to their heterogeneity and varying analysis section lengths an axle-centered energetic averaging over 21 adjacent spectral estimates was performed for each axle. The axles considered had to be at least 30 m away from an axle of a different wagon type and 60 m away from the end of the train. At least 26 and up to 158 axles were determined this way per type and barrier configuration (speeds from 72 to 100 km/h). For the reference cross-section the time points for the spectra were spaced similarly, taking into account differences in speed.

The spectra of the barrier cross-section were divided by the respective spectra of the reference cross-section. For the nearer microphones up to 7.5 m the emission microphone at the reference cross-section was used. For 25 m the immission position was used. The arithmetic mean of the so determined attenuation terms was then calculated over passbys or axles in the case of freight trains.

3 Results

3.1. Measurements

Fig. 3 shows the differences between the absorbing and the respective reflecting condition for all nine microphone positions as a function of frequency in terms of the one-third octave band center frequencies. Positive values imply a decrease in barrier attenuation for mounted panels. It is obvious, that there is a clear effect of the reflecting panels which is highly dependent on the measurement position. There are also differences between the panel configurations of up to 2 dB for the same number of panels. Reducing the reflecting surface reduces the adverse effect on the attenuation considerably.

3.2. Model calculations

Fig. 4 shows the comparison between BE calculations and measurements for six of the nine microphone positions. Shown is the top reflecting barrier compared to the absorbing barrier. Different source positions are color coded. Clearly, all source positions yield results comparable to the measurements across all microphone positions with some degree of over- or underestimation. Fig. 5 shows the same for the middle reflecing panels.

Figure 3: Measured reduction in attenuation for passenger train. Different settings are color coded. Dashed lines show the standard error of the mean. Positive values indicate a reduction in attenuation when using reflecting panels compared to a fully absorbing barrier.

Here, the omnidirectional wheel source (red lines) leads to an overestimate of the effect of the reflecting panels whereas the rail source (green lines) still yields a good agreement with the measurements. Using the mean absorption of the panels and the barrier also leads to a similar agreement with the situation where only every other panel was mounted. Using a horizontal dipole source at the wheel position (blue lines) in general leads to a further overestimation. This is most likely due to the horizontal directivity which leads to a higher weighting of positions close to the measurement cross-section, where the effect of multiple reflections is stronger.

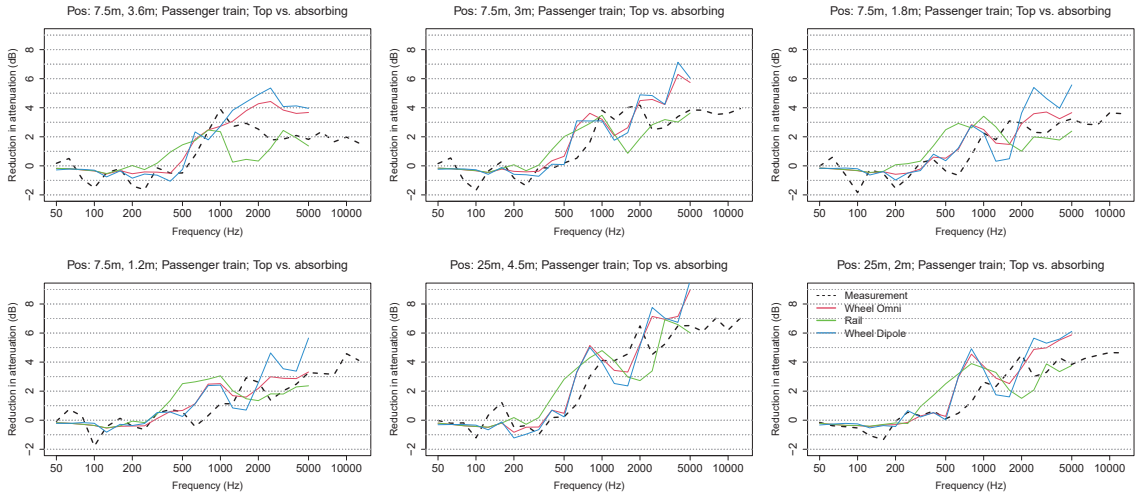

Figure 4: Measured and simulated reduction in attenuation for the top reflecting barrier compared to the fully absorbing barrier for the passenger train. The panels illustrate different microphone positions. Thin colored lines show calculation results for different source positions.

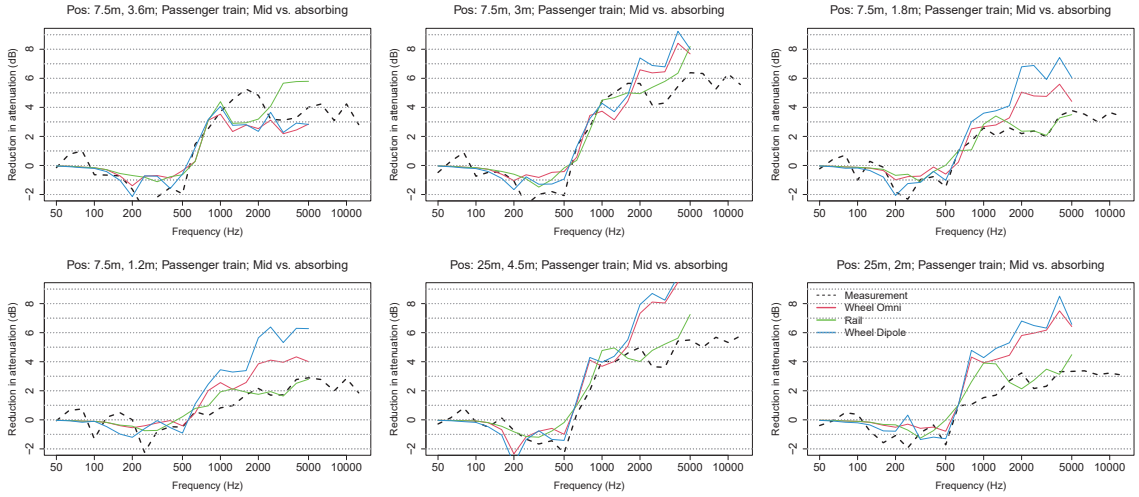

Figure 5: Measured and simulated reduction in attenuation for the middle reflecting barrier compared to the fully absorbing barrier for the passenger train. The panels illustrate different microphone positions. Thin colored lines show calculation results for different source positions.

As mentioned, there were two main types of commuter trains operating on the track. Both trains had a similar total length and height. The main difference between the two trains was that one type had a slightly curved vehicle body cross-section (referred to as commuter train 2). Looking at commuter train 1 (flat exterior), the measurement and calculation results are partially in good agreement (middle panel configuration in Fig. 6). The cross-section used for the calculations was very similar to the one for the passenger train. Gray dashed lines show the measurement results of the passenger train for comparison. Again, positioning the source at the center of the wheel leads to a considerable overestimation of the effect of the reflecting panels. Note, that the wheel source was positioned 50 mm lower due to the smaller wheels of the commuter trains.

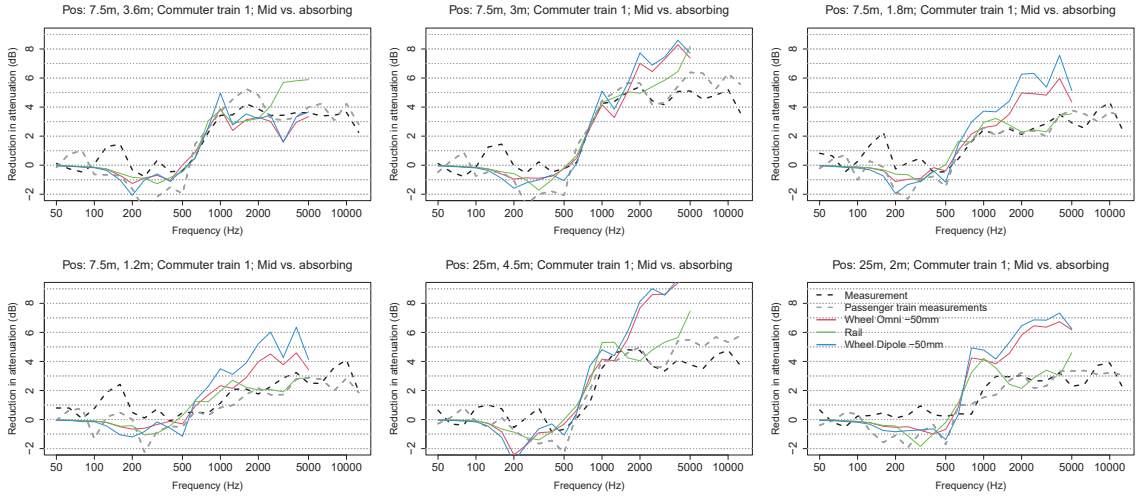

Figure 6: Measured and simulated reduction in attenuation for the middle reflecting barrier compared to the fully absorbing barrier for commuter train 1. The panels illustrate different microphone positions. Thin colored lines show calculation results for different source positions.

In contrast, for the commuter train 2 the panels caused a considerably smaller effect for all placements across most microphone positions (black vs. gray dashed lines in Figs. 7 and 8). For the top panel placements (Fig. 7),

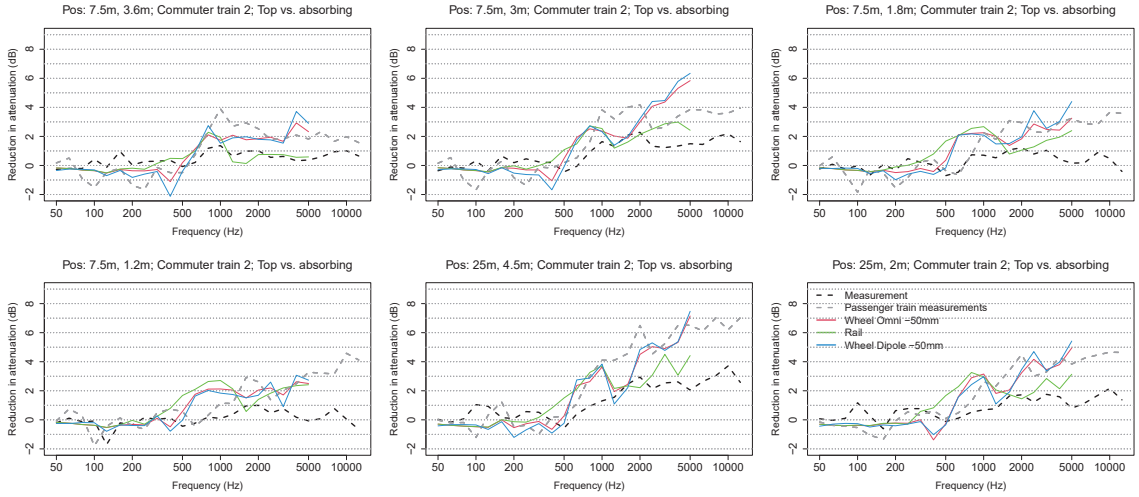

Figure 7: Measured and simulated reduction in attenuation for the top reflecting barrier compared to the fully absorbing barrier for commuter train 2. The panels illustrate different microphone positions. Thin colored lines show calculation results for different source positions.

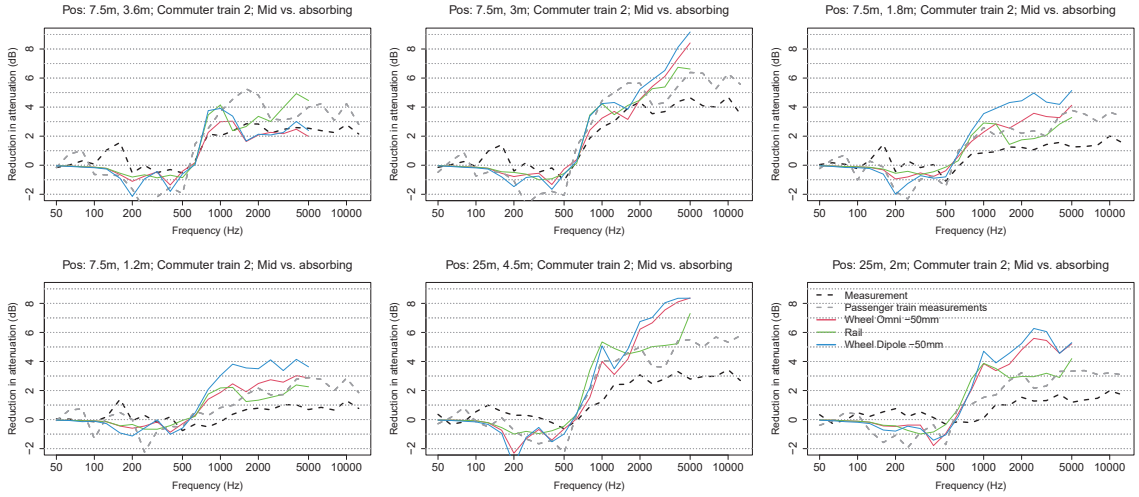

Figure 8: Measured and simulated reduction in attenuation for the middle reflecting barrier compared to the fully absorbing barrier for commuter train 2. The panels illustrate different microphone positions. Thin colored lines show calculation results for different source positions.

the effect is reduced by up to 4 dB compared to the passenger train. Even though the curved vehicle body was considered in the simulations for this train type, all source positions lead to an overestimation of the panel effect. Again, the source positioned on top of the rail leads to a better agreement. For the middle panels (Fig. 8) the reduction of the effect of the reflecting panels is up to 3 dB compared to the passenger train. Overall, the results for the calculations with the curved vehicle body were more similar to the passenger train.

Fig. 9 summarizes the findings for the passenger train and the commuter trains. Clearly, positioning the source at the rail (gray boxes) leads to an overall better agreement of simulations and measurements with a smaller median deviation as well as a smaller range of deviation indicated by reduced inter-quartile ranges. For commuter train 2 the overestimation at high frequencies is also clearly visible. The data presented also include the alternating panel configuration. For the alternating variant the approach using an average absorption coefficient also seems

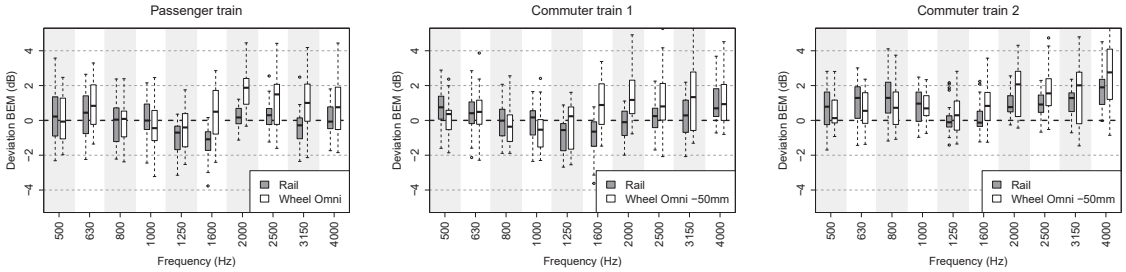

Figure 9: Deviation of simulations from measurements. Each panel shows the deviation of the simulations across microphones and variants (top, middle, and alternating reflecting panels) as a function of source position and frequency for the passenger train and the two commuter trains. The shading of the boxes indicates the source position. Only the omnidirectional sources are shown. Positive values imply an overestimation of the panel effect in the calculation.

to lead to similar agreements as for the top and middle variant.

Compared to passenger trains (including commuter trains) which have a mostly constant and known cross-section, freight trains vary much more in shape and can in practice only be modeled using rough estimations of the vehicle body. Here, results for extreme deviations from the box-shaped passenger train are shown: a flat wagon without any load, i.e., a wagon with essentialy no acoustically relevant vehicle body and a tank wagon with a circular cross-section (Fig. 10).

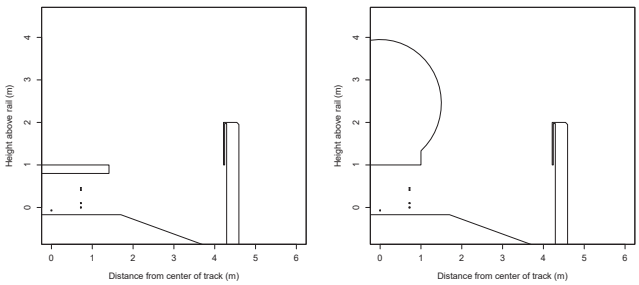

Figure 10: Cross-sections used for the simulation of freight trains. The left panel shows the flat freight wagon without load, the right panel a tank wagon.

Fig. 11 illustrates the results for a train comprising flat wagons without load (i.e. presumably without any acoustically relevant vehicle body for top reflecting panels, left panel in Fig. 10). As was to be expected, neither measurements nor simulations exhibit any significant effect of the reflecting panels.

As an extreme deviation from the box-shaped exterior of many passenger trains, tank wagons were also considered. As the exact exterior could not be acquired, a rough estimate of the diameter was done from the videos recordings (right panel in Fig. 10). The reflecting panels have less effect than for a box-shaped exterior, in particular for the middle panel position and elevated microphone positions (Fig. 12). Although, the calculations agree for most of the microphone positions, for the high position in 25 m, the results for the different panel positions are slightly contradictory, as the rail position leads to a good agreement for the top (not shown) and the wheel position leads to a good agreement for the middle position (Fig. 12). Positioning the source in between (100 mm above the top of the rail or 50 mm lower than the large wheel) leads to intermediate result.

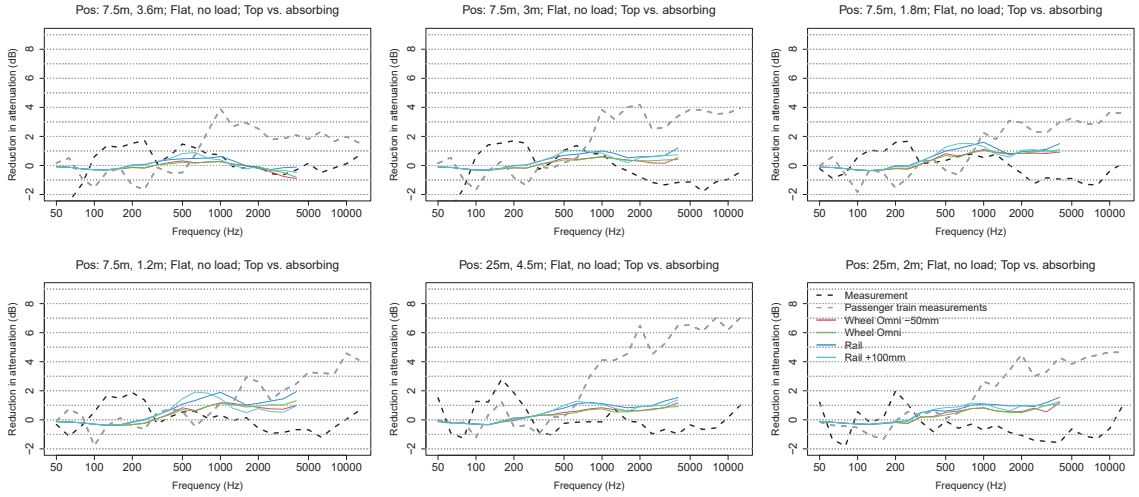

Figure 11: Measured and simulated reduction in attenuation for the top reflecting barrier compared to the fully absorbing barrier for flat freight wagons without load. The panels illustrate different microphone positions. Thin colored lines show calculation results for different source positions.

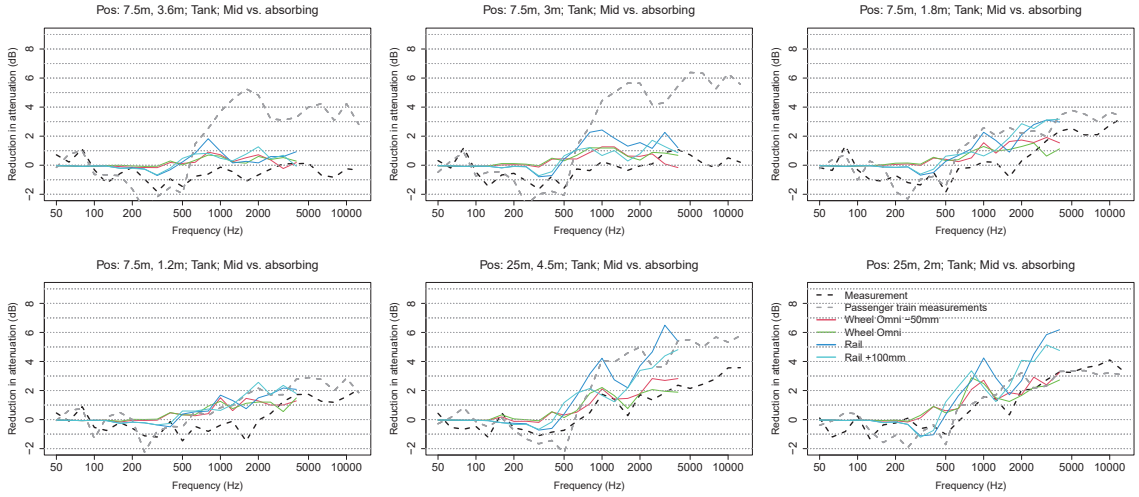

Figure 12: Measured and simulated reduction in attenuation for the middle reflecting barrier compared to the fully absorbing barrier for tank wagons. The panels illustrate different microphone positions. Thin colored lines show calculation results for different source positions.

4 Conclusions

Summarizing, the data illustrate that the panel positioning as well as the the train type have a considerable influence on the effect of reflective elements on a noise barrier. The exact reasons for the influences are not entirely clear. For commuter train 2, which has a slightly rounded shape which was taken into account in the simulations, the comparison between measurements and simulations showed larger deviations than for the passenger train and commuter train 1. Thus, the shape seems to be only a part of the reason for the altered effect of reflecting panels. Preliminary simulations show that the deviations between measurements and simulations when only rolling noise is used can be explained to a large degree by an additional source on top of the train (e.g. air conditioning units).

Overall, the 2.5D boundary element method provides a good tool to investigate such specific research questions. Considering the uncertainties present in in-situ passby measurements the agreement with the measured data is in parts very good with median deviations mostly below 1 dB. For the alternating panel configuration the simplifying assumption of an average absorption coefficient turned out to be sufficient for the situations considered here.

Using this calculation model, the current work is to simulate a large number of different settings (barrier heights, panel placement, train types) and compare the results to noise mapping calculations in order to identify any potential shortcomings of the currently used prediction method.

Acknowledgements

This work was in part supported by the Austrian Research Promotion Agency (FFG, project 873177), the Federal Ministry for Climate Action, Environment, Energy, Mobility, Innovation and Technology, and the Austrian Federal Railways (ÖBB-Infrastruktur AG).

References

[1] C. Kirisits, H. Meidl, G. Dinhobl, H. Gutschelhofer, J. Punk, and H. Kirisits. Comparison of measurements and calculations to investigate the effect of multiple-reflections between absorptive noise barriers and trains. In *Proceedings of Internoise*, 2013.

[2] European Union. Directive 2002/49/EC of the European Parliament and of the Council, 2021.

[3] P. Morgan, D.C. Hothersall, and S.N. Chandler-Wilde. Influence of Shape and Absorbing Surface—a Numerical Study of Railway Noise Barriers. *Journal of Sound and Vibration*, 217(3):405–417, 1998.

[4] C. Bustos, V. Jurdic, C. Sharp, and D. Hiller. Optimisation of Railway Noise Barrier Design Using Finite Elements and Boundary Element Modelling Methods. In *Euronoise 2021*, pages 390–399, 2021.

[5] C.H. Kasess, W. Kreuzer, and H. Waubke. An efficient quadrature for 2.5D boundary element calculations. *Journal of Sound and Vibration*, 382:213–226, 2016.

[6] D. Duhamel. Efficient calculation of the three-dimensional sound pressure field around a noise barrier. *Journal of sound and vibration*, 197(5):547–571, 1996.

[7] R.A. Broadbent, D.J. Thompson, and C.J.C. Jones. The acoustic properties of railway ballast. In *Euronoise*, pages 3307–3316, 2009.

[8] J. Smardzewski, T. Kamisiński, D. Dziurka, R. Mirski, A. Majewski, A. Flach, and A. Pilch. Sound absorption of wood-based materials. *Holzforschung*, 69(4):431–439, 2015.

[9] C.H. Kasess, H. Waubke, M. Conter, C. Kirisits, R. Wehr, and H. Ziegelwanger. The effect of railway platforms and platform canopies on sound propagation. *Applied Acoustics*, 151:137–152, 2019.

[10] C. H. Kasess, T. Maly, P. Majdak, and H. Waubke. The relation between psychoacoustical factors and annoyance under different noise reduction conditions for railway noise. *The Journal of the Acoustical Society of America*, 141(5):3151–3162, 2017.

[11] S.M.B. Fard, H. Peters, N. Kessissoglou, and S. Marburg. Modelling the acoustic performance of a noise barrier with a quasi-periodic boundary condition. In *Proceedings of the Forum Acusticum*, 2014.

[12] Z. Průša, P.L. Søndergaard, N. Holighaus, C. Wiesmeyr, and P. Balazs. The Large Time-Frequency Analysis Toolbox 2.0. In Mitsuko Aramaki, Olivier Derrien, Richard Kronland-Martinet, and Sølvi Ystad, editors, *Sound, Music, and Motion*, Lecture Notes in Computer Science, pages 419–442. Springer International Publishing, 2014.